This article has been accepted for publication in a future issue of this journal, but has not been fully edited. Content may change prior to final publication.

Simulations of an OSNR-Limited All-Optical Wavelength Conversion Scheme

Seán P. Ó Dúill, Sepideh T. Naimi, Aravind P. Anthur, Tam N. Huynh, Deepa Venkitesh, and Liam P. Barry

***Abstract*— We present simulations of a scheme to perform wavelength conversion of signals that eliminates phase-noise transfer from the pump to the converted signal. Nondegenerate four-wave mixing in a semiconductor optical amplifier is used to convert the signal to a new wavelength; and if an optical comb generator is used as the multiple-pump source, then the signal can be converted without incurring any phase-noise transfer from the pumps. We highlight the capabilities of this scheme by simulating the conversion of 16-QAM signals at 10 Gbaud and showing that errors due to phase-noise accumulation are eliminated thus enabling conversion whose only impairment would be the total additive optical noise.**

***Index Terms*—Semiconductor optical amplifiers, Wavelength conversion, Advanced modulation formats, Packet-switched networks.**

I. Introduction

To address the capacity crunch in wavelength division multiplexed (WDM) optical networks, rapid reconfigurable optical packet/burst switching technology in combination with advanced modulation formats, such as differential quadrature phase shift keying (DQPSK) and 16-quadrature modulation (QAM), would allow for the amplified spectral-bands of the fiber to be used more efficiently with high throughput. These future networks will require all-optical wavelength conversion to avoid contention in a node when two signals on the same wavelength are being switched to the same output fiber, thus improving network efficiency under heavy loads by fully utilizing all the available WDM channels [1]. A typical packet switched network is shown in Fig. 1. Data packets originating at the edge routers can be efficiently routed through the core network by dynamically altering the carrier wavelength of each packet at each core router to maximize the overall network capacity.

In order to perform wavelength conversion operations on DQPSK and 16-QAM signals, a coherent nonlinear process, such as four-wave mixing (FWM), is required to preserve the original amplitude and phase information. FWM, being transparent to modulation format, is also transparent to the signal baudrate; with conversion of 100 Gbit/s On-Off Keyed pulses having been demonstrated in semiconductor optical amplifiers (SOA) [2]. However, FWM has one major drawback and that is the issue of the large phase-noise transfer between the pump and the converted idler [3]. For the cases of degenerate and nondegenerate FWM, it is known that the linewidth transfer to the idler is 4 times that of the pump linewidth and the summation of the pump linewidths, respectively [3]. This issue is of crucial importance when converting formats such as 16-QAM signals using FWM because the increased phase uncertainty at the receiver degrades the overall system performance. Most of the recent works in the area of wavelength conversion of 16-QAM signals using nondegenerate FWM in SOAs, i.e. using two pump lasers [4],[5], have relied upon using separate pump lasers with linewidths around 100 kHz, and demonstrate good performance for single-stage wavelength conversion. To circumvent the phase-noise transfer problem, recently it was shown for the conversion of DQPSK signals [6], that if the two pumps are coherent, i.e. both pumps possess the same phase noise, then the DQPSK signal could be converted without incurring any phase-noise transfer from the pumps. Pumps with correlated phase noise could be derived from optical comb generators (OCG), which are optical sources containing many spectral lines with equidistant frequency spacing and the lines possessing correlated phase-noise; examples of which would be: mode locked lasers [6]; sinusoidally modulated single-mode lasers such as gain-switched lasers [7] and cascaded optical phase modulators [8]. In this letter, we use Monte Carlo simulations to evaluate the performance of the OCG-based nondegenerate FWM

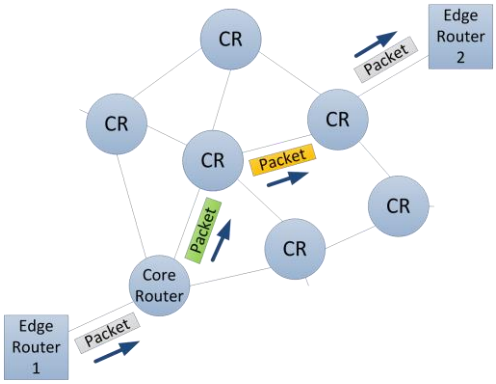

Fig. 1 Schematic of a typical wavelength-labeled packet switched network. A data packet, originating at edge router 1 and destined for edge router 2, undergoes wavelength conversion at each intermediary node to improve the network throughput at each core router.

This work was supported by the Science Foundation Ireland PI Program under grant number: (09/IN 1/12653).

S. Ó Dúill, S. T. Naimi, T. N. Huynh and L. P. Barry are with the Rince Institute, Dept. of Electronic Engineering, Dublin City University, Dublin 9, Ireland (e-mail: sean.oduill@dcu.ie).

A. P. Anthur and D. Venkitesh are with the Dept. of Electrical Engineering, Indian Institute of Technology Madras, Chennai 600036, India.

Copyright (c) 2013 IEEE. Personal use is permitted. For any other purposes, permission must be obtained from the IEEE by emailing pubs-permissions@ieee.org.

This article has been accepted for publication in a future issue of this journal, but has not been fully edited. Content may change prior to final publication.

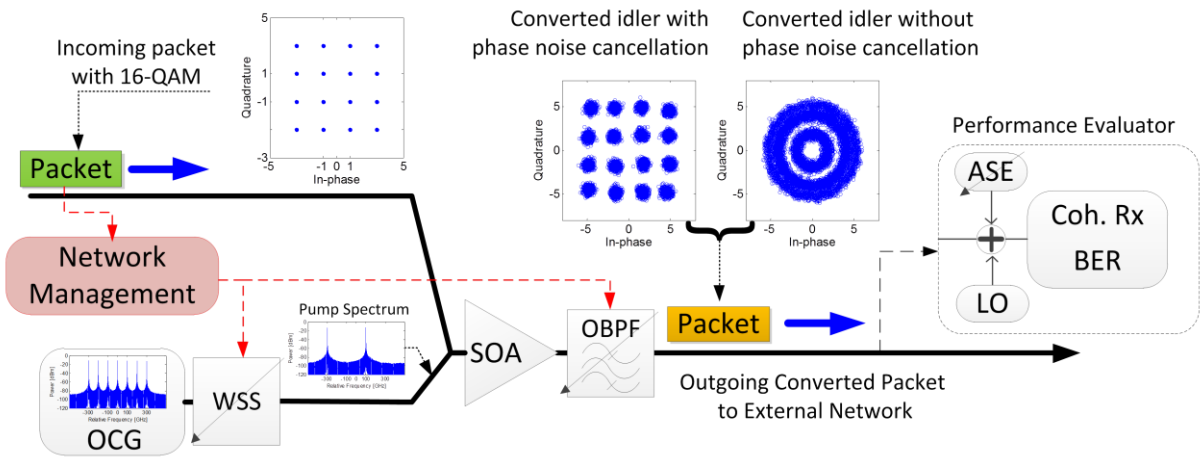

Fig. 2 System schematic of the FWM conversion scheme. Conversion of 16-QAM signals are depicted using detected constellations from the simulations. The constellations of the idlers with and without phase noise cancellation are shown to highlight the phase noise transfer (or lack thereof). The phase noise transfer from pump to idler wave results in a rotation of the constellations. The OBPF bandwidth is 10 GHz.

wavelength conversion technique for the conversion of 16-QAM signals. We implement a time domain SOA model and filter out the converted idler waves. The performance of the scheme is measured by employing actual error counting statistics. The wavelength conversion approach is different than that in [6], we are simulating a variation of the nondegenerate FWM scheme that allows for the conversion of the input signal to any wavelength within the SOA gain bandwidth; whereas in [6] the signal was up and down converted by the frequency difference between two pumps created by carrier-suppressed amplitude modulation in a Mach-Zehnder modulator.

The calculated bit error rate (BER) results show that the converted signal shows almost identical performance to the back-to-back performance of the original signal even when the linewidth of a single comb line is 10 MHz; thus proving that the scheme works regardless of the level of phase noise on the pumps, provided both pump lines have correlated phase-noise. In addition, evaluating the performance of the idler waves that experience phase noise transfer from the pumps allows us to infer the maximum tolerable pump linewidth for the conversion of 16-QAM signals using independent pump sources, i.e. two separate laser sources. Taking consideration that the signal may require multiple wavelength conversions to traverse the network, we estimate that a necessary condition for three consecutive wavelength conversion cascades (using independent pumps) for 16-QAM at 10 Gbaud could require pumps with linewidths <330 kHz. Therefore for practical purposes in constructing reconfigurable wavelength converters, only an OCG pump source could deliver reliable conversion of advanced modulation format signals with relaxed linewidth requirements due to correlated phase noise. It should also be noted that although the work undertaken in this letter employs an SOA, the benefits of employing dual correlated pumps to avoid phase noise transfer from the pumps to the converted signal is equally applicable to all third order nonlinear media such as highly nonlinear fiber and nonlinear waveguides.

II. Phase Noise Reduction Scheme

An outline of the scheme is shown in Fig. 2. Dual pumps with correlated phase-noise can be created by filtering out appropriate spectral lines from an OCG [6] with the assistance of a wavelength selective switch (WSS). Based on the wavelength of the incoming packet and the wavelength to which the packet is being converted to, the network management controls the WSS to filter the two specific pump lines from the OCG. The two pumps (P1 and P2) are then coupled with the incoming packet (denoted S for signal). The packet and pumps pass through the SOA and the signal is converted through FWM; the idler adapts to the same information encoded in the original packet and is then filtered out using an optical bandpass filter (OBPF) that is also under the tutelage of the network management. The converted packet is then transmitted to the next node. In order to evaluate the performance of the conversion scheme we detect the idler and

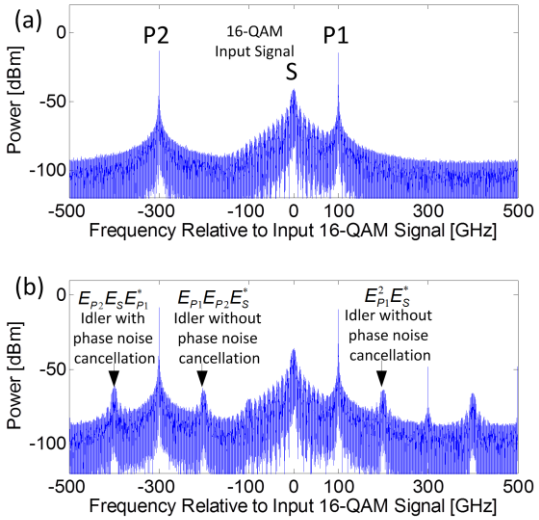

Fig. 3 Calculated: (a) Input spectrum showing signals and the two pumps. (b) Output spectrum indicating the idlers. Pump linewidth = 10 MHz. The spectral resolution is of the order of 100 kHz giving the illusion of weak pumps.

Copyright (c) 2013 IEEE. Personal use is permitted. For any other purposes, permission must be obtained from the IEEE by emailing pubs-permissions@ieee.org.

This article has been accepted for publication in a future issue of this journal, but has not been fully edited. Content may change prior to final publication.

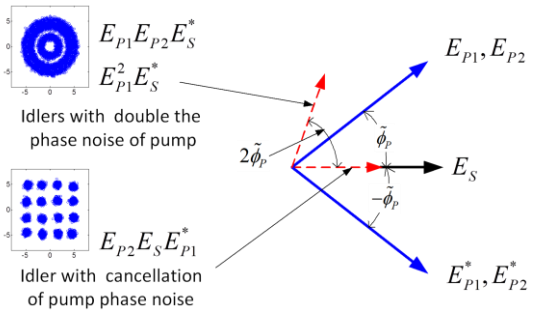

Fig. 4 Schematic of the phase noise transfer using vectors of the slowly-varying amplitudes of the pumps, signal and idler waves. The idler that does not experience phase noise transfer from the pumps is a scaled version of the original signal.

measure the BER. The coherent receiver (Coh. Rx.) block employs homodyne detection with a local oscillator (LO) and a controlled amount of noise loading, amplified spontaneous emission (ASE), is used to calibrate the optical signal to noise ratio (OSNR). ASE generated from the SOA is not included and is assumed to be lumped in with the general noise loading term. The 16-QAM signal is demodulated with the aid of an adaptive symbol normalizer and a tuned, decision-directed 1st order phase-locked loop (DD-PLL) to optimize the BER performance [10].

The input and output spectra of the SOA are shown in Fig. 3 with the various converted idlers of interest indicated in Fig.3 (b). The various idlers are extracted from the output field using a Gaussian-shaped OBPF. We adopt the following naming convention for the various idlers (indicated in Fig. 3(b)), $E_iE_jE_k^*$, where i, j and k denote the seeding pumps or signal i.e. P1, P2 or S; [*] denotes the complex conjugation operator. In addition to the possibility of minimizing the phase-noise transfer, another benefit of employing nondegenerate FWM lies in the reasonably constant conversion efficiency of the generated idlers irrespective of the frequency difference between P1 and P2 [11]. In the example shown here, the FWM conversion efficiency is determined mainly by the strength of the dynamic gain and index grating caused by the beating between S and P1; idlers ($E_{P2}E_SE_{P1}^*$ and $E_{P2}E_{P1}E_S^*$) are created due to the scattering of P2 from this gain and index grating. P2 could be placed anywhere within the gain bandwidth of the SOA, allowing for wide-band wavelength conversion [11].

The phase-noise cancellation concept is visualized in Fig. 4. The slowly varying envelopes of the pumps, signal and idler waves are plotted as vectors. The pumps possess correlated phase-noise $\tilde{\phi}_p$; also shown is the complex conjugate of the pumps to aid the visualization of the angles of the idlers. The nondegenerate idler that experiences phase-noise cancellation is $E_{P2}E_SE_{P1}^*$, because phase-noise from the pumps cancels due to the conjugation of one of the pumps [6] and this idler is an exact scaled copy of the original signal as shown in Fig. 4. In our simulation framework, this idler appears at a spectral location -400 GHz relative to the input signal in Fig. 3(b). The other two idlers, $E_{P2}E_{P1}E_S^*$ and $E_{P1}^2E_S^*$ do not experience phase-noise cancellation [6], and the phase-noise transfer they experience from the pumps is a doubling of $\tilde{\phi}_p$, hence a quadrupling of the pump linewidth [3]. We evaluate their performance to gain an insight into the scenario when separate pump sources are employed. In general when separate pump sources are used, the linewidth transfer is only the summation of the pump linewidths [3] because the phase-noise is uncorrelated.

III. Simulator

All our results were obtained from Monte Carlo simulations. In order to significantly reduce the simulation run-time, we implemented a lumped time-domain SOA model [12] operating on the slowly-varying envelope of the input optical field. As mentioned above, the main FWM generating gain and index grating is created by the signal S and a pump P1. The detuning between P1 and S is 100 GHz; therefore consideration of the carrier dynamics suffices to calculate all the idlers. The intraband effects [13], namely carrier heating and spectral hole burning, are not included in the analysis; though their omission only affects the absolute amplitude of the converted idlers and not the phase noise transfer. The lumped SOA gain dynamics are described by [12]:

$$\tau_S\dot{h} = h_0 - h(t) - P_{sat}^{-1}\left[\exp\{h(t)\}-1\right]\left|E_{in}(t)\right|^2 \qquad (1)$$

where the second term on the right hand side of (1) describes SOA gain depletion due to stimulated emission and the first term describes gain recovery back to the unsaturated value. The net unsaturated SOA gain, $\exp(h_0)$, was 17 dB, gain recovery time τ_S = 100 ps and saturation power P_{sat} = 10 mW. The pump linewidth was modeled as a random Weiner process [14], with phase-error variance over a time interval, $(t_1 - t_2) = \tau$, being: $\sigma_\phi^2 = 2\pi B_L\tau$ where B_L is the pump linewidth. The slowly varying envelope of the input optical field E_{in} is:

$$E_{in}(t) = \sqrt{P_{P1}}\exp\left(j\left(\Omega_{P1}t + \tilde{\phi}_P\right)\right) + \sqrt{P_{P2}}\exp\left(j\left(\Omega_{P2}t + \tilde{\phi}_P\right)\right) + \sqrt{P_S}E_S(t)\exp\left(j\tilde{\phi}_S\right) \qquad (2)$$

With the powers of P1 and P2 = 1 mW. $\tilde{\phi}_P$ is the correlated phase noise on both pumps, $\tilde{\phi}_S$ is the phase noise of the input signal and is uncorrelated with $\tilde{\phi}_P$. The average power of the 16-QAM signal is 100 μW. The carrier frequency of the signal is taken to be the reference frequency in all our simulations; the spectral placement of the input 16-QAM signal (packet) and both pumps are shown in Fig. 3(a). The input optical field, E_{in}, is created using (2), and then the SOA gain can be calculated using (1); the output field is thus given by:

$$E_{out}(t) = \exp\left\{\tfrac{1}{2}\left[-\alpha_{loss}L + (1 + j\alpha_H)h(t)\right]\right\}E_{in}(t) \qquad (3)$$

with the internal SOA losses, $\alpha_{loss}L$ = 2, and the gain-phase coupling (linewidth-enhancement) α_H -factor =4.

IV. Results.

We modulated a 10 Gbaud 16-QAM signal onto a carrier with a nominal linewidth of 10 kHz and then combined this signal with two CW pumps filtered from an OCG. The reason for creating a signal with low phase-noise is to explicitly indicate the role of phase-noise transfer from the pumps to the idlers. The linewidth of the pumps was set to 500 kHz and 1 MHz. Owing to the excellent performance for $E_{P2}E_SE_{P1}^*$, we show

Copyright (c) 2013 IEEE. Personal use is permitted. For any other purposes, permission must be obtained from the IEEE by emailing pubs-permissions@ieee.org.

This article has been accepted for publication in a future issue of this journal, but has not been fully edited. Content may change prior to final publication.

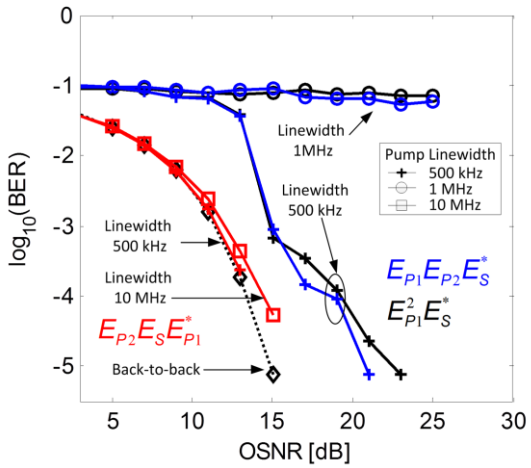

Fig. 5 Simulated BER results for each of the converted idlers for different pump linewidths. The red lines show the case of the idler that experiences no phase noise transfer from the pumps $E_{P2}E_SE_{P1}^*$. The other two idlers $E_{P2}E_{P1}E_S^*$ (blue curves) and $E_{P1}^2E_S^*$ (black lines) show significant OSNR penalty for a pump linewidth of 500 kHz.

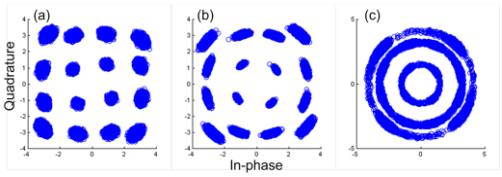

Fig. 6 Simulated constellations after applying the PLL for (a) $E_{P2}E_SE_{P1}^*$, pump linewidth = 10 MHz; (b) $E_{P2}E_{P1}E_S^*$, pump linewidth = 500 kHz and (c) $E_{P},E_{P1}E_S^*$, pump linewidth = 1 MHz.

the result using an OCG with 10 MHz linewidth alongside the result for 500 kHz (see red lines in Fig. 5). The performance is measured by calculating the BER versus OSNR employing 2^{17}-1 symbols (4x[2^{17}-1] bits for 16-QAM); allowing us to generate a statistically significant number of errors for BERs >10^{-5}. Setting the OSNR at the output helps visualize the OSNR penalty with respect to the back-to-back scenario. The calculated BER versus OSNR curves for each idler are shown in Fig. 5. As expected, the idler corresponding to $E_{P2}E_SE_{P1}^*$ shows the best performance, incurring a slight OSNR penalty due to spectral leakage from the pumps when the linewidth is 10 MHz as compared to 500 kHz. The other idlers, $E_{P2}E_{P1}E_S^*$ and $E_{P1}^2E_S^*$, exhibit similar poor BER performance hence the > 5 dB OSNR penalty to offset the errors caused by the phase-noise transfer when the pump linewidth is 500 kHz. The conversion scheme ultimately fails for these idlers using pumps with 1 MHz linewidth.

The detected constellations after the PLL for $E_{P2}E_SE_{P1}^*$ and $E_{P2}E_{P1}E_S^*$ with various pump linewidths are shown in Fig. 6. The detected constellation for $E_{P2}E_SE_{P1}^*$ shows only a slight degradation caused by inevitable SOA gain saturation due to the multilevel amplitude 16-QAM signal. The detected constellations of $E_{P2}E_{P1}E_S^*$ clearly exhibit phase-noise transfer, as is evident from the increased rotation of the detected constellations. When the pump linewidth is 500 kHz, the DD-PLL begins to have difficulty in tracking and correcting for the transferred phase-noise, and completely fails to unravel the 16-QAM constellation for 1 MHz pump linewidth. From Fig. 5 we can estimate the linewidth requirements for using separate pump lasers from these results. Based on the >5 dB OSNR penalty at a BER of 10^{-5} for a pump linewidth of 500 kHz; a single stage converter using separate pumps would require the pump linewidth to be <1 MHz (as discussed at the end of Section II), the scalability of employing multiple-cascaded FWM-based wavelength converters for 16 QAM signals would require linewidths of separate pump lasers to be < 330 kHz for 3 cascades. However, no such linewidth limit exists when deriving correlated pumps from an OCG thus rendering the conversion scheme to be dependent upon OSNR accumulation and could enable the conversion of advanced modulation format signals with reliable performance.

V. Conclusions

We simulated wavelength conversion of 16-QAM signals using FWM in a SOA, without phase-noise transfer. Our results show the absence of a BER floor imposed by the lack of phase noise transfer even when employing pumps with 10 MHz linewidth showing that the performance is limited by the accumulated OSNR. The use of this technique could enable practical all-optical wavelength conversion in next generation optical packet/burst switched networks.

VI. References

[1]. G. K. Chang, J. Yu, Y. K. Yeo, A. Chowdhury, and Z. Jia, "Enabling technologies for next-generation optical packet switching networks," *Proc. Of the IEEE*, **94**, No. 5, pp 892 -910, (2006).

[2]. A. E. Kelly, A. D. Ellis, D. Nesset, and R. Kashyap, "100 Gbit/s wavelength conversion using FWM in an MQW semiconductor optical amplifier," *Electron. Lett.* **34**, No. 20, pp. 1955 -1956, (1998).

[3]. R. Hui and A. Mecozzi, "Phase Noise of Four-wave Mixing in Semiconductor Lasers," *Appl. Phys. Lett.* **60**, pp 2454-2456 (1992).

[4]. G. Contestabile, Y. Yoshida, A. Maruta, and K. Kitayama, "Ultra-broad band, low power, highly efficient coherent wavelength conversion in quantum dot SOA", *Opt. Expr*. **20**, No. 25, pp. 27902-27907, (2012).

[5]. B. Filion, S. Amiralizadeh, A. T. Nguyen, L. A. Rusch, and S. LaRochelle, "Wideband wavelength conversion of 16 Gbaud 16-QAM signals in a semiconductor optical amplifier," *Proc. of opt. fib. comm. conf.* OFC'13, OTh1C.5, (2013).

[6]. A. Anthur, R. Watts, J. O'Carroll, D. Venkitesh, and L. P. Barry, "Dual correlated pumping scheme for phase noise preservation in all-optical wavelength conversion," *Opt. Expr*., **21**, 13, pp. 15568-15579 , (2013).

[7]. H. Haus, "Mode locking of lasers," *IEEE J. of Select Topics in Quant. Electron.***6**, No. 6, pp 1173 – 1185, (2000).

[8]. P. Anandarajah, R. Zhou, R. Maher, D. Gutierrez-Pascual, F. Smyth, V. Vujicic, and L. P. Barry, "Flexible optical comb source for super channel systems," *Proc. of* OFC'13, OTh3I.8, (2013).

[9]. T. Healy, F. Gunning, A. D.Ellis, J. D. Bull, 'Multi-wavelength source using low drive-voltage amplitude modulators for optical communications'. *Opt. Expr*., **15**, No. 6, pp 2981-2986, (2007).

[10]. S. J. Savory, "Digital coherent optical receivers: algorithms and subsystems," *IEEE J. of S. Top. in Quant. Electron*. **16**, 5, 1164, (2010).

[11]. I. Tomkos, I. Zacharopoulos, D. Syvridis,a) T. Sphicopoulos, and C. Caroubalos "Improved performance of a wavelength converter based on dual pump four-wave mixing in a bulk semiconductor optical amplifier," *Appl. Phys. Lett*., **72**, No. 20, pp 2499 - 2501, (1998)

[12]. G. P. Agrawal and N. A. Olsson, "Self-phase modulation and spectral broadening of optical pulses in semiconductor laser amplifiers," *IEEE J. of Quant. Electron.*, **25**, No. 11, 2297, (1989).

[13]. G. P. Agrawal, "Population pulsations and nondegenerate four-wave mixing in semiconductor lasers and amplifiers "*J. of Opt. Soc. Am. B*, **5**, No. 1, pp 147 -159, (1988).

[14]. D. Marcuse, "Computer simulation of FSK laser spectra and of FSK-to-ASK conversion," *IEEE J. of Lightw. Techn*. **8**, No. 7, 1110, (1990).

Copyright (c) 2013 IEEE. Personal use is permitted. For any other purposes, permission must be obtained from the IEEE by emailing pubs-permissions@ieee.org.